Proc. Natl. Acad. Sci. USA
Vol. 95, pp. 1230–1235, February 1998
Microbiology

A family of chimeric erythrocyte binding proteins of malaria parasites

(*Plasmodium berghei*/*Plasmodium yoelii yoelii*/apical membrane antigen 1/rhoptry/merozoite)

STEFAN H. I. KAPPE, AMY R. NOE, TRESA S. FRASER, PETER L. BLAIR, AND JOHN H. ADAMS*

Department of Biological Sciences, University of Notre Dame, Notre Dame, IN 46556-5645

Communicated by Louis H. Miller, National Institute of Allergy and Infectious Diseases, Bethesda, MD, November 25, 1997 (received for review August 5, 1997)

ABSTRACT **Proteins sequestered within organelles of the apical complex of malaria merozoites are involved in erythrocyte invasion, but few of these proteins and their interaction with the host erythrocyte have been characterized. In this report we describe MAEBL, a family of erythrocyte binding proteins identified in the rodent malaria parasites *Plasmodium yoelii yoelii* and *Plasmodium berghei*. MAEBL has a chimeric character, uniting domains from two distinct apical organelle protein families within one protein. MAEBL has a molecular structure homologous to the Duffy binding-like family of erythrocyte binding proteins located in the micronemes of merozoites. However, the amino cysteine-rich domain of MAEBL has no similarity to the consensus Duffy binding-like amino cysteine-rich ligand domain, but instead is similar to the 44-kDa ectodomain fragment of the apical membrane antigen 1 (AMA-1) rhoptry protein family. MAEBL has a tandem duplication of this AMA-1-like domain, and both of these cysteine-rich domains bound erythrocytes when expressed *in vitro*. Differential transcription and splicing of the *maebl* locus occurred in the YM clone of *P. yoelii yoelii*. The apical distribution of MAEBL suggested localization within the rhoptry organelles of the apical complex. We propose that MAEBL is a member of a highly conserved family of erythrocyte binding proteins of *Plasmodium* involved in host cell invasion.**

Malaria merozoites enter erythrocytes by an active invasion process mediated by parasite ligands interacting with erythrocyte receptors (1, 2). Within minutes after release into the blood a free merozoite must recognize and enter an erythrocyte to ensure maintenance of the blood-stage infection. Mediators of the invasion process are positioned on the merozoite surface and in the organelles of the apical complex (micronemes, rhoptries, dense granules) when the merozoites mature in the schizont (3).

A key step early in host cell invasion and a principal determinant of host cell specificity is the irreversible commitment of the merozoite to the selected host cell by the formation of a junction between merozoite and erythrocyte (4, 5). Junction formation is mediated by the Duffy binding-like (DBL) family of homologous erythrocyte binding proteins (EBPs) located within the micronemes of merozoites. The DBL-EBP family includes the *Plasmodium vivax*/*Plasmodium knowlesi* Duffy antigen binding proteins (DBPs) and the *Plasmodium falciparum* erythrocyte binding antigen 175 (EBA-175) (6–8). The similarity among DBL-EBPs is most prominent in two cysteine-rich domains, designated amino cysteine-rich domain and carboxyl cysteine-rich domain (6). The amino cysteine-rich domain is the principal adhesion domain binding to the erythrocyte receptors (9, 10), but the carboxyl cysteine-rich domain has no clear function, although the high degree of amino acid conservation among *Plasmodium* species suggests that this domain is important.

Apical membrane antigen 1 (AMA-1) is a highly conserved apical organelle protein (11) thought to be involved in a receptor–ligand interaction during the merozoite invasion of erythrocytes prior to receptor recognition by DBL-EBPs. AMA-1 is a transmembrane protein initially located within the rhoptry organelles of developing merozoites and is subsequently released onto the surface of invasive merozoites after proteolytic processing into a noncovalently linked 44-kDa (44/42-kDa doublet) fragment and a 22-kDa transmembrane fragment (12–14) .

In this report, we complete the isolation of recently identified *dbl-ebp* genetic elements from *P. yoelii yoelii* and *Plasmodium berghei* (15). Surprisingly, these genes encode proteins that have a chimeric character, showing homology to DBL-EBPs in the carboxyl cysteine-rich domain and identity to AMA-1 within the amino cysteine-rich domains. We demonstrate that both of the amino cysteine-rich domains have erythrocyte binding activity. Thus we conclude that this apical organelle protein family, named MAEBL, represents a new branch in a superfamily of malaria parasite adhesion molecules.

MATERIALS AND METHODS

Parasites, DNA and RNA Preparation. BALB/c mice were inoculated intraperitoneally with *P. berghei* ANKA, and ICR mice were inoculated intraperitoneally with *P. yoelii yoelii* YM (World Health Organization reference clones). Parasitized blood was collected from infected animals and passed through a leukocyte removal column (Baxter). Genomic DNA was extracted by a chloroform/phenol method. Total RNA was isolated by using the Ultraspec RNA isolation system (Biotecx Laboratories, Houston).

Southern Blot Analysis. Parasite genomic DNA was digested with restriction enzymes *Acc*I, *Bam*HI, *Eco*RI, or *Hin*dIII, separated by agarose gel electrophoresis, fragmented in 0.25 M HCl, denatured in 0.5 M NaOH/1.5 M NaCl, and blotted as described previously (7). The blot was hybridized first with a cDNA clone that did not contain the 3′ region, and then with a reverse transcriptase (RT)-PCR product extending

The publication costs of this article were defrayed in part by page charge payment. This article must therefore be hereby marked "*advertisement*" in accordance with 18 U.S.C. §1734 solely to indicate this fact.

Abbreviations: AMA-1, apical membrane antigen 1; DBL, Duffy binding-like; DBP, Duffy antigen binding protein; EBP, erythrocyte binding protein; EBA-175, erythrocyte binding antigen 175; GST, glutathione *S*-transferase; HSVgD1, herpes simplex virus glycoprotein D1; IFA, indirect immunofluorescence assay; RBC, red blood cell; RT, reverse transcriptase.

Data deposition: The sequences reported in this paper have been deposited in the GenBank database (accession nos. AF031886 and AF031887).

*To whom reprint requests should be addressed. e-mail: adams.20@nd.edu.

from the beginning of the carboxyl cysteine-rich domain to the stop codon. Both probes were radiolabeled by random priming by using the Klenow fragment of DNA polymerase (BRL). The blot was then incubated in a final wash of 0.2× SSC/0.5% SDS (1× SSC = 0.15 M sodium chloride/0.015 M sodium citrate, pH 7.0) at 60°C and the membrane was exposed to a DuPont NEF-496 film for 48 hr at −70°C. The blot was stripped between hybridizations by boiling it in 0.1× SSC/1% SDS for 30 min.

Northern Blot Analysis. Total parasite RNA was enriched for poly(A)-RNA, and 2 μg was separated by agarose gel electrophoresis and blotted by using standard techniques. The blot was hybridized overnight with the same probes as described for Southern blot analysis, incubated in a final wash of 0.1× SSC/0.1% SDS at 42°C, and exposed as described above. The blot was stripped between hybridizations in 50% formamide/4× SSPE/1% SDS (1× SSPE = 0.18 M sodium chloride/10 mM sodium phosphate/1 mM EDTA, pH 7.4) at 65°C for 3 hr.

Genomic and cDNA Cloning. Genomic DNA of *P. yoelii yoelii* YM was digested with *Eco*RI, ligated into plasmid pcDNA3 (Invitrogen), and used to transform *Escherichia coli* TOP10F′ by electroporation. Colony lifts (Magna Lift, Micron Separations) were screened with a radiolabeled PCR fragment representing the 3′ region of *P. yoelii yoelii maebl* as described for Southern blot hybridizations. The cDNA was prepared by using a ZAP Express cDNA synthesis kit (Stratagene), ligated into plasmid pUC18, and used to transform *E. coli* TOP10F′. Colony lifts were screened with a radiolabeled *maebl* genomic clone. Oligonucleotide primers matching the *P. yoelii yoelii* YM cDNA clone amplified the corresponding regions from *P. berghei* DNA. Fragments were cloned into plasmid pCRII (Invitrogen) for sequencing.

DNA Sequencing and Sequence Analysis. The nucleotide sequences of cloned DNA were determined by the dideoxynucleotide chain termination method (Pharmacia Biotech). Nucleic acid and deduced amino acid sequences were aligned by using the ALIGNMENT algorithm (Geneworks 2.2, IntelliGenetics). Similar sequences were searched for in GenBank by using the BLAST algorithm (16).

RT-PCR. Total RNA of *P. yoelii yoelii* YM treated with DNase I (GIBCO/BRL) was used as template in RT-PCR (Perkin–Elmer) with the oligonucleotide primers (214 sense, 5′-ATACGTACTGGGTACCTTAAC-3′; 278 antisense, 5′-GACCTAAACAATAATTTTGA-3′; 279 antisense, 5′-CTATATAATGAACAATCAAG-3′; Fig. 4).

Cos-7 Cell Surface Expression and Erythrocyte Binding Assay. The *P. yoelii yoelii* YM *maebl* regions encoding the M1 and M2 domains were PCR amplified separately by using oligonucleotide primers flanking each region (M1; 297 sense, 5′-ata*cagctg*GATAACCCACAAGAAGATTTTATG-3′; 299 antisense, 5′-ata*gggccc*ATAGTGAGTTGGAGCATTCGTATT-3′. M2; 300 sense, 5′-ata*cagctg*CCTAATCCTCAAGCCGAATATATG-3′; 301 antisense, 5′-ata*gggccc*AAAATGTTCAGGAGCACTATTATG-3′; bases shown in lowercase were added to facilitate directional cloning into plasmid pRE4, and the *Pvu*II and *Apa*I restriction cleavage sites are in italics). The plasmid pRE4 (17) was utilized to express heterologous sequences encoding putative MAEBL binding domains as chimeras with herpes simplex virus glycoprotein D1 (HSVgD1) on the surface of COS-7 cells. Recombinant plasmids were purified by using an endotoxin-free plasmid purification kit (Qiagen, Chatsworth, CA). Plasmids (2 μg per well or chamber) were transfected into COS-7 cells, grown on chamber slides or in 35-mm well plates, by using Lipofectin (GIBCO/BRL). Surface expression was detected by indirect immunofluorescence assay (IFA) using monoclonal antibodies 1D3 or DL6 against HSVgD1 epitopes remaining in the expression construct (17). Binding assays were carried out by using a 10% mouse red blood cell (RBC) suspension in RPMI medium 1640 added onto tranfected cells 48 hr after transfection. Incubation was done for 2 hr at room temperature. Cells were washed four times very gently with PBS to remove nonadherent RBCs. Binding was scored by counting rosettes in 30 fields of 200× magnification. Rosettes were counted as positive when adherent RBCs covered more than 50% of the cell surface. Untransfected cells and a *P. vivax* region II construct (10) were used as controls in binding assays and IFA.

Preparation of Glutathione *S*-Transferase (GST) Fusion Proteins. Two GST fusion proteins were prepared: the first fusion protein (A7) represented part of the M2 amino cysteine-rich domain of *P. yoelii yoelii* YM MAEBL and was generated with two oligonucleotides located within this region (214 sense, 5′-gaaggatccATACGTACTGGGTACCTTAAC-3′; 215 antisense, 5′-cttggatccaagctttcaGATTCATCGGTATTTCTTGTAG-3′). The second fusion protein, described previously (15), represented the carboxyl cysteine-rich domain of MAEBL. Bases shown in lowercase were added to facilitate directional cloning into plasmid pGEX2T (18). The PCR products were inserted in frame into plasmid pGEX2T. Fusion proteins were purified on glutathione Sepharose 4B (Pharmacia) and eluted with reduced glutathione.

Polyclonal Serum Preparation and IFA. Polyclonal immune serum to GST fusion proteins was prepared in rabbits as previously described (15). Affinity-purified antiserum was prepared by adsorbing polyclonal serum to strips of nitrocellulose covered with fusion protein overnight at 4°C. Strips were agitated 1 hr at room temperature in PBS containing 0.05% Tween-20 (PBS-T) and then washed for 10 min in boric acid buffer (100 mM boric acid/150 mM NaCl, pH 9.0) to reduce unspecific binding. The nitrocellulose strips were washed again in PBS-T for 10 min, and bound antibodies were eluted for 30 min at room temperature in 200 mM glycine/150 mM NaCl, pH 2.8. Eluents were neutralized to pH 7.0. *P. yoelii yoelii* YM blood stage parasites were washed 3 times in RPMI medium 1640, fixed 5 min with RPMI medium 1640/1% formaldehyde at 37°C, lysed in buffer (RPMI medium 1640/0.1% saponin/0.1% fetal bovine serum) and then processed for IFA as described previously. Samples were viewed under a MRC-1024 laser scanning confocal imaging system (Bio-Rad).

RESULTS

Primary Structure of the *P. yoelii yoelii* YM *maebl*. An 8-kb *Eco*RI genomic fragment was isolated from *P. yoelii yoelii* YM that contained the coding region for the consensus DBL-EBP carboxyl cysteine-rich domain. This genomic clone represented a single-copy gene (Fig. 1) and the region encoding the DBL-EBP carboxyl cysteine-rich domain was identical to a

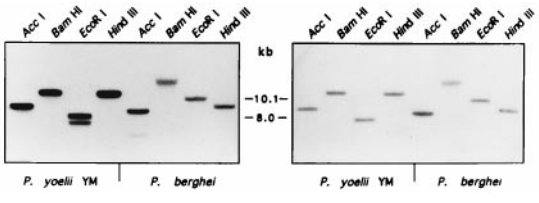

FIG. 1. Southern blot hybridizations of *P. yoelii yoelii* and *P. berghei,* demonstrating that *maebl* is a single-copy chimeric gene. Genomic DNA was hybridized with a *P. yoelii yoelii* YM cDNA clone (5′ region) encoding only the AMA-1-like domains (*Left*) and a probe specific for the 3′ region of *maebl* encoding the EBP-like region (*Right*). Both probes hybridized to the same single restriction fragments, except when the restriction site was within the nucleotide sequence of the probe (*Acc*I for *P. berghei* and *Eco*RI for *P. yoelii yoelii* YM). Differences in signal intensity represent differences in the size of the nucleic acid probes. Fragment sizes are given in kilobases as calculated on the basis of λ/*Hin*dIII molecular markers. Restriction endonucleases *Acc*I, *Bam*HI, *Eco*RI, and *Hin*dIII are indicated over each lane.

323-bp PCR-amplified element previously identified from *P. yoelii yoelii* YM (15). The deduced amino acid sequence and the exon/intron structure at the 3′ end of the gene were elucidated by comparing genomic sequence to RT-PCR products (data not shown). The consensus DBL-EBP carboxyl cysteine-rich domain was followed by a predicted transmembrane domain encoded by a single exon and a putative cytoplasmic domain encoded by two exons. This 3′ part of the gene fragment was very similar to a previously characterized *P. berghei* gene fragment, and both are homologous to the *P. vivax*/*P. knowlesi dbp*s and the *P. falciparum eba-175* (Fig. 2). Upstream of the carboxyl cysteine-rich coding region was a 1,400-bp region encoding 13-residue tandem repeats rich in lysine and glutamic acid. Although this repetitive region was similar in length to the corresponding regions of the DBPs and EBA-175, its amino acid sequence was not similar.

As expected on the basis of the consensus DBL-EBP structure, a cysteine-rich domain preceded the repeat region. Surprisingly, this cysteine-rich domain encoded by the *P. yoelii yoelii* gene had no similarity to the consensus DBL domains of the *P. vivax*/*P. knowlesi* DBPs or the *P. falciparum* EBA-175. Instead, this cysteine domain had partial, but significant, identity with subdomains 1 and 2 of the *Plasmodium* AMA-1, corresponding to the 44-kDa extracellular domain fragment (19). This new gene family has been named *maebl* because its deduced structure is chimeric, being like both AMA-1 and DBL-EBP.

The 8-kb genomic fragment did not appear to represent the complete gene coding sequence of *maebl* because the ORF of the genomic fragment began at the *Eco*RI cloning site, there was no signal peptide, and there was not an initiation of translation site. This was confirmed by two identical 5.6-kb cDNA clones that were independently isolated from different *P. yoelii yoelii* YM cDNA libraries screened with the genomic clone as a probe, forming a contig with the genomic clone and

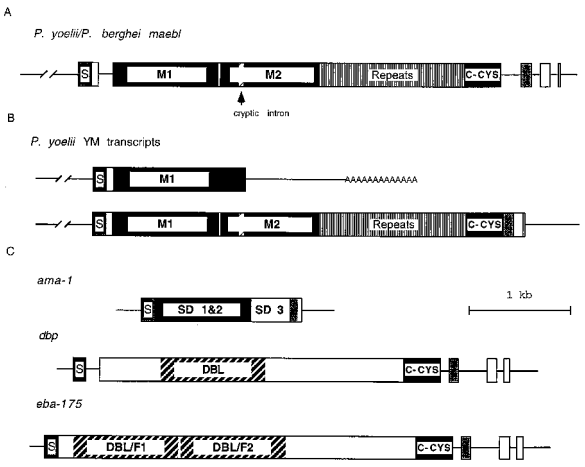

FIG. 2. Comparison of the gene structures of *maebl, dbl-ebps,* and *ama-1*. Coding sequences are boxed and drawn to scale and horizontal lines represent introns and untranslated regions. (*A*) Schema representing the genomic structure of *P. yoelii yoelii* and *P. berghei maebl*. Exon 1 encodes the signal peptide (S); exon 2 encodes the AMA-1-like cysteine-rich domains (M1, M2), the repeat region (REPEATS), and the DBL-EBP carboxyl cysteine-rich domain (C-CYS); exon 3 encodes a transmembrane domain; and exons 4 and 5 encode the cytoplasmic tail. The cryptic intron (indicated by the arrow) is identified at the beginning of M2. (*B*) Schemata of the 5.6- and 8.0-kb transcripts of *P. yoelii yoelii* YM *maebl*. The large transcript encompassed all exons, but the small transcript terminated within the region encoding the repeats. (*C*) Schemata of *ama-1, dbp,* and *eba-175* are shown for comparison with *maebl*. The first two AMA-1 subdomains (SD 1 & 2) together correspond to each MAEBL AMA-1-like cysteine-rich domain (M1, M2). The relative similarity of the M1 and M2 domains was reminiscent of the similarity of the F1 and F2 domains of EBA-175.

completing the 5′ ORF. A start codon was preceded by a Kozak initiation of translation site and a 1.95-kb 5′ untranslated region. A putative signal sequence was followed by a tandem repeat of two AMA-1-like cysteine-rich domains (designated M1 and M2). The deduced amino acid sequences of these two domains had 40% sequence identity (Table 1), suggesting an origin by duplication.

The MAEBL M1 and M2 domains had significant deduced amino acid sequence similarity with the *P. yoelii yoelii* AMA-1 (Fig. 3). All 10 cysteines of AMA-1 subdomains 1 and 2 were conserved within the *P. yoelii yoelii* MAEBL cysteine-rich domains and additional similarity was greatest for the residues adjacent to these cysteines (similarity of ≥15 in a PAM-250 matrix) (20). Differences between MAEBL and AMA-1 were found mostly in the loop regions between predicted AMA-1 disulfide bridges. In the region corresponding to the first two loops of AMA-1 subdomain 1, MAEBL had a large unique segment with 6 cysteine residues not present in the consensus AMA-1 structure. In contrast, the MAEBL region corresponding to the AMA-1 subdomain 2 was truncated. There was no similarity between MAEBL and the third AMA-1 subdomain. The protein encoded by the complete ORF was predicted to have a molecular mass of 200 kDa.

The complete genomic structure of the *P. yoelii yoelii maebl* locus was elucidated by comparing overlapping PCR-amplified genomic fragments to the cloned cDNA. Two introns were identified in the 5′ portion of *maebl* (Fig. 2 *A* and *B*); the first intron, 120 bp, followed the putative signal sequence and a second, cryptic, intron, 95 bp, was found within the beginning of the M2 domain. Removal of this second intron created an ORF shift so that translation would be terminated shortly downstream of the splice junction. This splicing event would result in the expression of a truncated form of the protein containing only the M1 domain and beginning of the M2 domain.

Primary structure of the *P. berghei maebl*. A *maebl* homologue was PCR-amplified from *P. berghei* by using oligonucleotide primers based on the *P. yoelii yoelii* YM *maebl*. Southern blot analysis of *P. berghei* confirmed that *maebl* is a single-copy gene (Fig. 1) and that the PCR-amplified gene fragments were contiguous with the previously cloned *ebp*-like genomic fragment (data not shown). The gene structure of the *P. berghei maebl* was identical to that of the *P. yoelii yoelii* YM *maebl* and the deduced amino acid sequences were highly similar (Table 1). All cysteine residues were conserved in number and position between the *P. berghei* and *P. yoelii yoelii* MAEBL (Fig. 3). The removal of the first intron following the putative signal sequence was verified by RT-PCR (data not shown), and sequencing showed that the exon splice junctions were conserved compared with the *P. yoelii yoelii* YM *maebl*.

Differential Transcription and Splicing of *maebl* Occurs in P. yoelii yoelii YM. Northern blot analysis of *P. yoelii yoelii* YM poly(A)-enriched RNA identified two major transcripts when the 5.6-kb cDNA clone (containing only the 5′ region of *maebl*) was used as a probe (Fig. 4*A*). A 5.6-kb transcript corresponded in size to the cDNA clones representing polyadenylated mRNAs and a larger transcript of about 8 kb corre-

Table 1. Pairwise comparison of deduced amino acid sequences between the M1 and M2 domains of the *P. yoelii yoelii* YM (PyYM) and the *P. berghei* (Pb) MAEBL and the AMA-1 of *P. yoelii yoelii* YM

	PyYM/M2	Pb/M1	Pb/M2	PyYM/AMA-1
PyYM/M1	40	90	35	20
PyYM/M2		39	72	19
Pb/M1			36	19
Pb/M2				18

Numbers are percent identity.

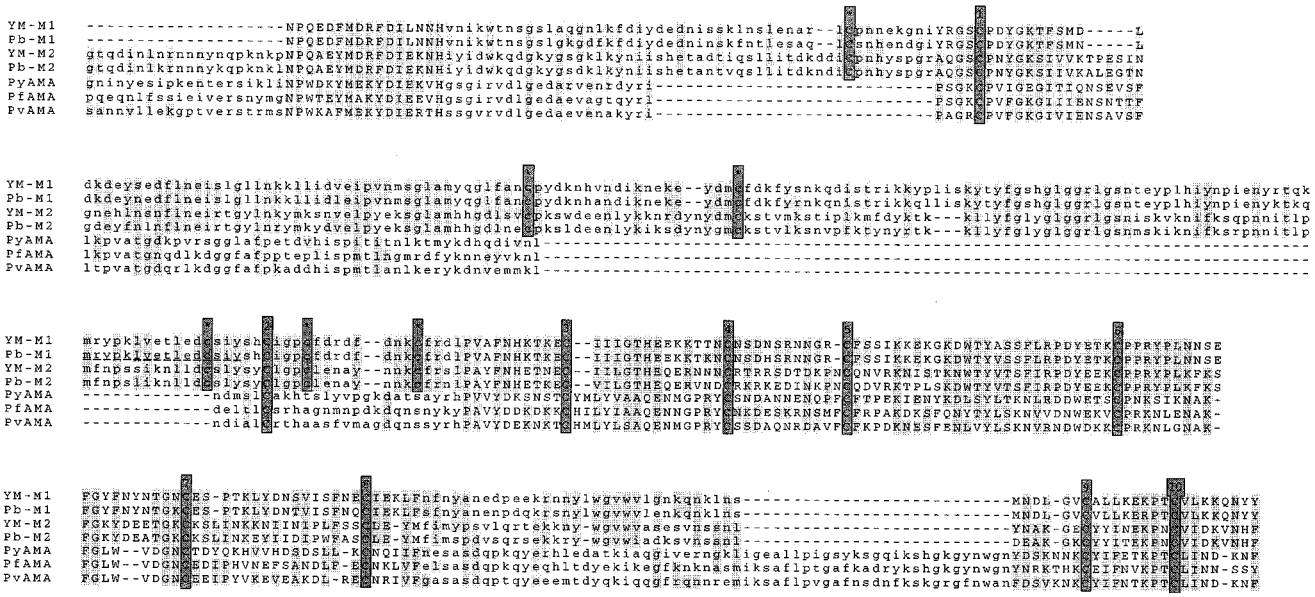

FIG. 3. Similarity of the MAEBL cysteine-rich domains M1 and M2 to AMA-1. Alignment of the M1 and M2 deduced amino acid sequences of *P. yoelii yoelii* YM (YM) and *P. berghei* (Pb) MAEBL compared with the first two AMA-1 subdomains of *P. yoelii yoelii* (Py), *P. falciparum* (Pf), and *P. vivax* (Pv). This part of AMA-1 corresponds to the 44-kDa fragment. All cysteine residues of the AMA-1 conserved in MAEBL are boxed and numbered as in AMA-1 (subdomain 1 = residues 1–6, subdomain 2 = residues 7–10); the deduced disulfide linkages are 1—6, 2—3, 4—5, 7—10, and 8—9 (19). Cysteine residues conserved only in MAEBL are marked by an asterisk. Blocks of significant sequence similarity are in capital letters, with shaded residues having similarity in both M1 and M2 or between MAEBL and AMA-1. Dashes indicate spaces inserted for best alignment.

sponded to the predicted size of the complete transcript of the coding sequence. To verify that the large transcript did encode the complete ORF, the Northern blot was stripped and rehybridized with a probe specific to only the 3′ region of *maebl*. This probe hybridized only to the 8-kb transcript (Fig. 4*B*), demonstrating that the large transcript encoded the complete protein, including the amino and carboxyl cysteine-rich domains, the transmembrane domain, and the cytoplasmic domain. The data indicate that the *P. yoelii yoelii* YM *maebl* locus is differentially transcribed. RT-PCR with two different oligonucleotide primer sets confirmed the presence of two different transcripts, one containing the cryptic intron, one lacking this intron (Fig. 4*C*). Because the 5.6-kb cDNA clones did not contain the cryptic intron it is likely that differential splicing is linked to the small transcript.

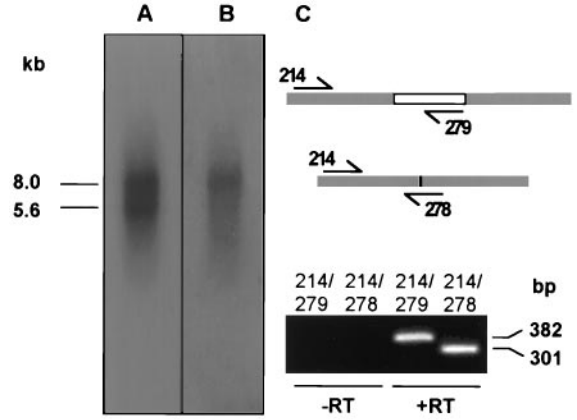

FIG. 4. Northern blot hybridizations and RT-PCR of *P. yoelii yoelii* YM RNA, demonstrating differential transcription and splicing of *maebl*. Poly(A)-enriched RNA of *P. yoelii yoelii* YM was hybridized with a *P. yoelii yoelii* YM cDNA clone encoding only the AMA-1-like domains (*A*) or a probe specific for the 3′ region of *maebl* encoding the EBP-like region (*B*). Two transcripts with apparent sizes of 8.0 kb and 5.6 kb were hybridized by the probe to the AMA-1-like encoding region, but the probe to the 3′ region of *maebl* hybridized only to the 8-kb transcript. This fact demonstrated that only the 8-kb transcript encoded the carboxyl cysteine-rich domain, the transmembrane domain, and the cytoplasmic tail. Transcript sizes are given in kilobases as calculated on the basis of a 0.24- to 9.5-kb RNA ladder. Brightness and contrast were adjusted electronically. (*C*) RT-PCR demonstrating differential splicing of *maebl* transcripts. The schema shows the cryptic intron within the region encoding the M2 domain and the oligonucleotide primer positions used for specific amplification. Primer combination 214/278 amplified a product from a transcript lacking the cryptic intron, and primer combination 214/279 amplified a product from a transcript containing the cryptic intron. No amplification could be detected in control reactions without RT (−RT).

Identification of the Erythrocyte Binding Domains of MAEBL. The position of the M1 and M2 domains within MAEBL suggested that these domains are the functional equivalents of the DBL ligand domains of EBA-175 and the DBPs. We reasoned that erythrocyte binding activity would likely reside within these MAEBL domains. The M1 or M2 domains were expressed as HSVgD1 fusion proteins on the surface of transfected COS-7 cells (Fig. 5*C*). Recombinant surface expression of the *P. yoelii yoelii* YM M1 or M2 domain resulted in rosetting of mouse RBCs but not of human RBCs on the surface of transfected cells (Fig. 5 *A* and *B*). In contrast, a construct expressing the *P. vivax* DBP region II bound human RBCs (10). The M2 domain was consistently more effective than the M1 domain in conferring binding activity to transfected COS-7 cells. The relative number of rosettes varied, but in experiments with comparable transfection efficiencies for both constructs, cells transfected with the M2 domain had 4- to 6-fold more rosettes than cells transfected with the M1 domain.

Immunolocalization of *P. yoelii yoelii* YM MAEBL. The M2 subdomain of the amino cysteine-rich domain and the carboxyl cysteine-rich domain of *P. yoelii yoelii* YM were expressed as separate GST fusion proteins. Both fusion proteins were used to produce polyclonal anti-*P. yoelii yoelii* sera in rabbits, anti-M2 (A7), and anti-YM C-CYS (YM2T/8), respectively. Anti-M2 serum reacted to the developing merozoite apical complex in segmenting schizonts in a pattern similar to that of the anti-YM C-CYS antibodies affinity purified on recombi-

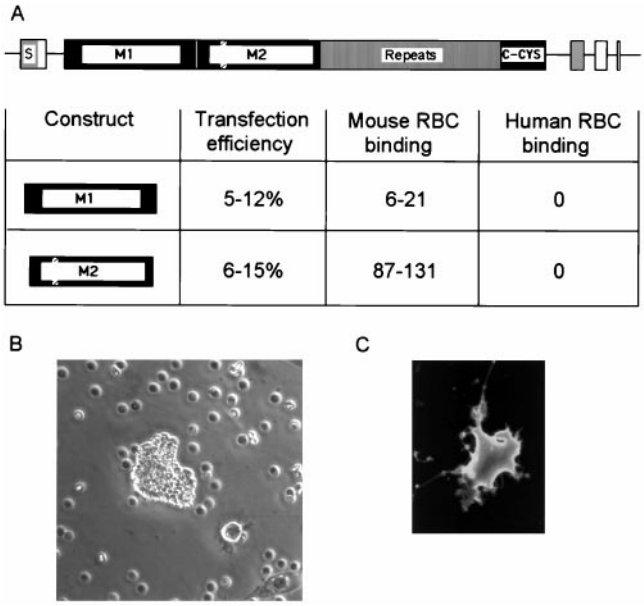

Construct	Transfection efficiency	Mouse RBC binding	Human RBC binding
M1	5-12%	6-21	0
M2	6-15%	87-131	0

FIG. 5. Expression of the M1 and M2 domains of the *P. yoelii yoelii* MAEBL on the surface of COS-7 cells leads to RBC rosetting. (*A*) Results of five independent RBC binding assays with M1 and M2 domain constructs. Expression of the M2 domain resulted in 4- to 6-fold more rosettes than expression of the M1 domain. No rosetting could be observed for the M1 and M2 domains with human RBCs. The numbers were derived by counting rosettes in 30 fields of 200× magnification. (*B*) Representative RBC rosette on a COS-7 cell transfected with the M2 domain. (×600.) (*C*) IFA with monoclonal antibody DL6, showing surface fluorescence of a COS-7 cell transfected with the M2 domain. (×600.)

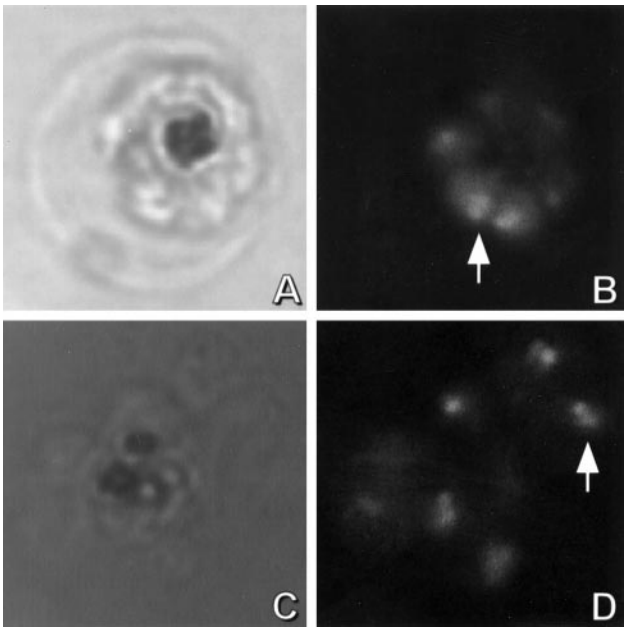

FIG. 6. Immunolocalization of MAEBL to the merozoite apical complex by using scanning confocal laser microscopy. (*B* and *D*) Immunofluorescence with antibodies to the AMA-1-like domain M2 (A7) (*B*) and the EBP carboxyl cysteine-rich domain (YM C-CYS) (*D*) both localized MAEBL to the merozoite apical complex of *P. yoelii yoelii* YM. *A* and *C* are the nonconfocal transmitted images of *B* and *D*, respectively. The immunofluorescence pattern with each antibody was characteristic of a rhoptry protein as demonstrated by the bilobed structure present in numerous merozoites (arrows). (×3000.)

nant C-CYS protein (Fig. 6). Antibodies to both proteins clearly reacted to a bilobed structure at the apical end of merozoites within late-stage schizonts. This bilobed fluorescence pattern is typically seen for proteins located within rhoptries, which are the prominent, pear-shaped, paired organelles of the apical complex. Previously, the anti-C-CYS sera also detected surface fluorescence on merozoites in late-stage schizonts (15). Both of these anti-YM MAEBL sera cross-reacted with the protein doublet previously identified from *P. berghei* (data not shown).

DISCUSSION

MAEBL represents a previously undescribed family of EBPs expressed in malaria merozoites. MAEBL is a chimeric molecule partly like a DBL-EBP and partly like AMA-1. Importantly, the ligand domains of MAEBL have identity to AMA-1 instead of the expected consensus DBL motif found in the corresponding location (region II) of the *P. vivax* DBP and the *P. falciparum* EBA-175 (Fig. 1). The DBL domain is the defining motif represented in a large superfamily of adhesive proteins, and this cysteine domain was demonstrated to be the principal determinant of receptor recognition for the DBL-EBP (9, 10) and for some *Plasmodium falciparum* erythrocyte membrane proteins 1 (21). Therefore, the AMA-1-like cysteine motif of MAEBL (M1, M2) appears as a functional replacement for the consensus DBL motif and defines another adhesive motif used by malaria parasites.

The basic gene structure of *maebl* conforms to that previously defined for the *dbl-ebp* family (6) and not that of *ama-1* (11, 12). *maebl* is a single-copy gene and has a multi-exon structure with each exon representing a functional domain: (*i*) signal, (*ii*) putative extracellular domain, (*iii*) transmembrane domain, and (*iv* and *v*) a cytoplasmic domain. The deduced amino acid sequence of the carboxyl cysteine-rich domain and the exon/intron boundaries at the 3′ end of *maebl* are homologous to those of *dbl-ebp*. Although the amino cysteine-rich region of MAEBL is not homologous to DBL-EBPs, its position relative to the carboxyl cysteine domain is equivalent. The repeat region, corresponding to DBL-EBP regions III–V, maintains a spacing between the amino and carboxyl cysteine domains similar in size to that found in the DBL-EBPs. AMA-1 is highly conserved among *Plasmodium* both at the nucleotide and amino acid level; it is encoded by a single ORF that varies only at the 5′ end. The structural characteristics of MAEBL suggest that this apical organelle protein serves a functional role in the merozoite more similar to a DBL-EBP than to AMA-1.

The AMA-1-like M1 and M2 domains of the *P. yoelii yoelii* YM MAEBL exhibited *in vitro* erythrocyte binding activity, similar to the DBL domains of *P. vivax, P. knowlesi,* and *P. falciparum* (9, 10). The M2 domain appears to be the principal ligand domain, because it showed more binding activity than did the M1 domain. Although the MAEBL receptor is not yet identified, receptor specificity of the M1 and M2 domains was demonstrated by binding of erythrocytes of the laboratory host but not of human erythrocytes.

Each AMA-1-like domain of MAEBL corresponds to the core structure of the AMA-1 44-kDa fragment (19), also suggesting an adhesive function for this fragment of AMA-1. Previous data suggested that this AMA-1 region was potentially important in a receptor–ligand interaction, because Fab fragments of monoclonal antibodies to conformational epitopes of the 44-kDa fragment competitively inhibited invasion of malaria merozoites (22).

The two different *maebl* transcripts expressed in the YM clone were a large transcript predicted to encode a full-length transmembrane protein and a short transcript predicted to encode a soluble product. Differential transcription of the short transcript was associated with the removal of a cryptic intron in the M2 domain that would shift the reading frame and

produce a putative soluble protein, representing the M1 domain, and analogous to the processed AMA-1 44-kDa domain. Differential splicing in higher eukaryotes is a common mechanism for producing alternate functional forms of a protein. An example is the switch between membrane-bound and secreted forms of immunoglobulins (23). Currently, we do not know what function a soluble M1 domain might serve during the invasion process.

MAEBL showed an apical expression and localization pattern within merozoites by IFA that was most consistent with being a rhoptry protein. MAEBL was also previously localized on the surface of mature merozoites, a characteristic shared with AMA-1. This contrasts markedly with the DBL-EBPs, which are sequestered in the micronemes, a separate apical organelle not connected to the rhoptries, and in addition have not been demonstrated on the surface of free merozoites (7, 8, 24).

MAEBL is an EBP of malaria parasites containing a novel adhesive motif for receptor recognition. It is, to our knowledge, the first chimeric *Plasmodium* molecule that has characteristic domains from two distinct apical organelle proteins. MAEBL is highly conserved not only in rodent malaria parasites but throughout the genus *Plasmodium*, as demonstrated by the identification of a *maebl* homologue in *P. falciparum* (unpublished data). We predict that MAEBL functions as an adhesion molecule important as a determinant or modifier of host cell specificity. The chimeric structure of MAEBL is consistent with the type of molecule that would function in an alternate invasion pathway parallel or redundant to the DBL-EBP.

We thank Drs. Gary Cohen and Roselyn Eisenberg for providing the plasmid pRE4 and the monoclonal antibodies 1D3 and DL6. This work was supported by the National Institutes of Health (Grant R29 AI33656) and the University of Notre Dame Faculty Research Program. J.H.A. is a recipient of a Burroughs Wellcome Fund New Investigator Award in Molecular Parasitology. A.R.N. and P.L.B. were supported by National Institutes of Health Experimental Parasitology and Vector Biology Training Grant AI07030.

1. Barnwell, J. W. & Galinski, M. R. (1995) *Ann. Trop. Med. Parasitol.* **89,** 113–120.
2. Galinski, M. R. & Barnwell, J. W. (1996) *Parasitol. Today* **12,** 20–29.
3. Holder, A. A., Blackman, M. J., Borre, M., Burghaus, P. A., Chappel, J. A., Keen, J. K., Ling, I. T., Ogun, S. A., Owen, C. A. & Sinha, K. A. (1994) *Biochem. Soc. Trans.* **22,** 291–295.
4. Aikawa, M., Miller, L. H., Johnson, J. & Rabbege, J. (1978) *J. Cell Biol.* **77,** 72–82.
5. Miller, L. H., Aikawa, M., Johnson, J. G. & Shiroishi, T. (1979) *J. Exp. Med.* **149,** 172–184.
6. Adams, J. H., Sim, B. K. L., Dolan, S. A., Fang, X., Kaslow, D. C. & Miller, L. H. (1992) *Proc. Natl. Acad. Sci. USA* **89,** 7085–7089.
7. Adams, J. H., Hudson, D. E., Torii, M., Ward, G. E., Wellems, T. E., Aikawa, M. & Miller, L. H. (1990) *Cell* **63,** 141–153.
8. Sim, B. K. L., Toyoshima, T., Haynes, J. D. & Aikawa, M. (1992) *Mol. Biochem. Parasitol.* **51,** 157–160.
9. Sim, B. K. L., Chitnis, C. E., Wasniowska, T. J., Hadley, T. J. & Miller, L. H. (1994) *Science* **264,** 1941–1944.
10. Chitnis, C. & Miller, L. H. (1994) *J. Exp. Med.* **180,** 497–506.
11. Waters, A. P., Thomas, A. W., Deans, J. A., Mitchell, G. H., Hudson, D. E., Miller, L. H., McCutchan, T. F. & Cohen, S. (1990) *J. Biol. Chem.* **265,** 17974–17979.
12. Peterson, M. G., Marshall, V. M., Smythe, J. A., Crewther, P. E., Lew, A., Silva, A., Anders, R. F. & Kemp, D. J. (1989) *Mol. Cell. Biol.* **9,** 3151–3154.
13. Narum, D. L. & Thomas, A. W. (1994) *Mol. Biochem. Parasitol.* **67,** 59–68.
14. Crewther, P. E., Culvenor, J. G., Silva, A., Cooper, J. A. & Anders, R. F. (1990) *Exp. Parasitol.* **70,** 193–206.
15. Kappe, S. H. I., Curley, G. P., Noe, A. R., Dalton, J. P. & Adams, J. H. (1997) *Mol. Biochem. Parasitol.* **89,** 137–148.
16. Altschul, S. F., Gish, W., Miller, W., Myers, E. W. & Lipman, D. J. (1990) *J. Mol. Biol.* **215,** 403–410.
17. Cohen, G. H., Wilcox, W. C., Sodora, D. L., Long, D., Levin, J. Z. & Eisenberg, R. J. (1988) *J. Virol.* **62,** 1932–1940.
18. Smith, D. B. & Corcoran, L. M. (1991) in *Current Protocols in Molecular Biology*, eds. Ausubel, F. M., Brent, R., Kingston, R., Moore, D., Seidman, J., Smith, J. & Struhl, K. (Wiley, New York), Vol. 2, pp. 16.7.1–16.7.8.
19. Hodder, A. N., Crewther, P. E., Matthew, M. L. S. M., Reid, G. E., Moritz, R. L., Simpson, R. J. & Anders, R. F. (1996) *J. Biol. Chem.* **271,** 29446–29452.
20. Dayhoff, M. O. & Eck, R. V. (1968) *Atlas of Protein Sequence and Structure* (Natl. Biomed. Res. Found., Washington, DC), Vol. 5.
21. Rowe, J. A., Moulds, J. M., Newbold, C. I. & Miller, L. H. (1997) *Nature (London)* **388,** 292–295.
22. Thomas, A. W., Deans, J. A., Mitchell, G. H., Alderson, T. & Cohen, S. (1984) *Mol. Biochem. Parasitol.* **13,** 187–199.
23. Early, P., Huang, H., Davis, M., Calame, K. & Hood, L. (1980) *Cell* **19,** 981–992.
24. Sim, B. K., Orlandi, P. A., Haynes, J. D., Klotz, F. W., Carter, J. M., Camus, D., Zegans, M. E. & Chulay, J. D. (1990) *J. Cell. Biol.* **111,** 1877–1884.